Theor Chem Acc (2000) 104:109–115
DOI 10.1007/s002140000112

Theoretical
Chemistry Accounts

Regular article

Topological approach in the structural and bonding characterization of lanthanide trihalide molecules

Laurent Joubert[1], **Bernard Silvi**[1], **Gérard Picard**[2]

[1] Laboratoire de Chimie Théorique (U.M.R 7616), Université Pierre et Marie Curie, 4 Place Jussieu, 75252 Paris Cedex 05, France
[2] Laboratoire d'Electrochimie et de Chimie Analytique (U.M.R. 7575), E.N.S.C.P., 11, rue Pierre et Marie Curie, 75231 Paris Cedex 05, France

Received: 1 July 1999 / Accepted: 17 November 1999 / Published online: 19 April 2000

Abstract. We present a systematic study of the structural and bonding properties of selected lanthanide trihalide molecules, LnX_3 (Ln = La, Gd or Lu, X = F or Cl). A topological analysis of the electron localization function has been carried out, revealing typical ionic bonding properties. The increasing ionic character of the Ln–X bonds through the rare-earth series has been clearly emphasized. Moreover, we have pointed out a strong distortion of the outer core shell of the metal. This singularity induces a typical tetrahedral arrangement of the lanthanide outer core basins, thus favoring a pyramidal equilibrium geometry. On the other hand, this structural effect is counterbalanced by increasing ligand repulsions through the series due to the well-known lanthanide contraction; therefore, these repulsions favor a planar arrangement of the molecular system with the appearance of a new core basin in the outer core shell of the metal.

Key words: Lanthanide trihalide molecules – Topological bonding analysis – Electron localization function – Density functional theory

1 Introduction

The last 3 decades saw growing interest in the chemistry of heavy element compounds, such as lanthanide or actinide derivatives [1–2]. In this particular domain, one of the most important fields of research concerns the study of lanthanide–ligand interactions for molecules that are or may be involved in nuclear waste treatment [3]. More particularly, pyrochemical techniques are now strongly envisaged to improve the actual chemical processes in the nuclear industry [4]. In this perspective, an experimental and theoretical research program is currently in progress in our laboratory, focusing on lanthanide fluoride and chloride properties [5–9]. From a theoretical point of view, we have recently reported quantum mechanics ab initio and density functional theory (DFT) studies [7, 8] on lanthanide trihalide vapor molecules, LnX_3 (La, Gd or Lu, X = F or Cl). These studies allowed us to assess the advantages and drawbacks of quantum chemistry methodology to predict structural and thermodynamic properties of heavy element derivatives. In particular, the assumption of the corelike behavior of f electrons has been checked. Another theoretical approach, which is based on molecular mechanics (MM) simulations, was the object of recent investigations by Gaune-Escard and coworkers [10, 11] on LnX_3 species in a molten salt environment. These studies, which rely on the widespread model of triply charged cations in pure electrostatic interaction with the coordinated ligands, have pointed out the inadequacy of this model to simulate the behavior of lanthanide halide molecules in ionic liquid media. Therefore, an accurate description of the corresponding bonding features is revealed to be a challenging task for the further determination of, for example, adequate MM force field parameters. Besides this particular aspect, the chemical description of these interactions remains a fundamental topic for a better understanding of the molecular properties of heavy element series.

The present article aims to provide an insight into the bonding properties of lanthanide trifluoride and trichloride vapor molecules. Although numerous experimental [12, 13] and theoretical [14] investigations have been carried out on these systems, bonding property studies are rather scarce in the literature [15–18]. Semiempirical work [15, 16] has suggested a strong covalent character for these trihalide salts, while no specific ab initio study has been realized on this particular topic. Nevertheless, this fundamental aspect has been developed in recent theoretical studies based on a hybrid DFT/Hartree–Fock (HF) approach [17, 18]. In the framework of the natural resonance theory (NRT) [19], Adamo and Maldivi [17] performed a detailed natural bond orbital (NBO) analysis [20]. While a simple Mulliken population analysis suggests that the Ln–X bonds

Correspondence to: L. Joubert,
e-mail: joubert@lct.jussieu.fr

have partial covalent character, NBO charges indicate, in contrast, strong ionic interactions for these systems, decreasing as expected with the increasing softness of the ligand. As underlined by these authors, chemical intuition strongly suggests an increase in the hardness of lanthanide cations through the rare-earth series, thus inducing and favoring ionic bonding interactions. It seems important to note that this qualitative trend has been confirmed by polarizability calculations [21], which predicted a decreasing polarizability of lanthanide cations through this series. Nevertheless, this aspect is not clearly evidenced by a NBO analysis that indicates, in contrast, decreasing ionic interactions from Gd to Lu derivatives. Similar trends are suggested by a coupled NBO/NRT approach, emphasizing the limitations of these methodologies. Another description of the nature of *Ln–X* bonds has been recently proposed by the same authors [18] thanks to a precise energetic analysis based on the transition-state method developed by Ziegler and Rauk [22]. The predominance of electrostatic bonding interactions has been clearly established, the variations of the ionic character being in good agreement with the increasing hardness of the metal. Here, we assess precisely and quantitatively the character of these bonding interactions with a modern analysis of chemical bonding, i.e. a topological analysis of the electron localization function (ELF). Moreover, we expect this topological analysis to explain the particular geometrical structure of these molecules, which remains a subject of controversy.

2 Methods of calculation

2.1 Computational details

All the calculations were performed on a SGI R10000 server (Origin 200) using the Gaussian 94 quantum chemical package [23]. A hybrid B3LYP DFT/HF approach [24–26] was employed to estimate the molecular wavefunction. A set of quasirelativistic effective core potentials was used [27, 28], including the *f* orbitals within the core orbitals with a fixed $4f$ occupation corresponding to the desired valency of the atom. Such core pseudopotentials are referred to as small core pseudopotentials because the electrons belonging to the external core shell, here $5s^25p^6$, are explicitly taken into account in the calculation as well as the valence electrons. In this framework, the rare-earth elements are modeled as 11-electron systems ($5s^25p^65d^16s^2$) described with optimized ($7s6p5d$)/[$5s4p3d$] valence basis sets. All-electron polarized 6-31G(d) basis sets were employed for fluorine and chlorine atoms. The equilibrium geometries as well as the cohesive energies, $E(LnX_3) - E(Ln^{3+}) - 3E(X^-)$ obtained in the present and in previous DFT calculations are given in Table 1.

These values are consistent with the structural and energetic analysis previously performed by Adamo and Maldivi [18]. Finally, our topological analysis was performed using the TopMod package [29] and the ELF2D program [30] and all the corresponding figures were produced using the data analyzer SciAn [31].

Table 1. Optimized bond lengths and bond angles (see Ref. [8] for computational details) and cohesive energies (this work) for the selected lanthanide trihalide molecules

Molecule	R (Å)	θ (°)	Cohesive energy (au) $E_{\text{cohesive}} = E(LnX_3) - E(Ln^{3+}) - 3E(X^-)$
LaF_3	2.14	110.8	−1.91
GdF_3	2.04	113.6	−2.01
LuF_3	1.97	116.0	−2.09
$LaCl_3$	2.65	118.1	−1.50
$GdCl_3$	2.53	118.8	−1.58
$LuCl_3$	2.44	119.9	−1.65

2.2 Topological analysis

The topological approach to chemical bonding was pioneered by Bader 3 decades ago and has been applied to the analysis of the electron density and its Laplacian, constituting the so-called "theory of atoms in molecules" [32]. More recently, Becke and Edgecombe [33] have proposed an ELF $\eta(r)$, which is defined as

$$\eta(r) = \frac{1}{1 + \left(\frac{D_\sigma}{D_\sigma^0}\right)^2} \quad , \tag{1}$$

where D_σ and D_σ^0 represent the curvature of the same spin electron pair density (Fermi hole) for the actual system and a reference homogeneous electron gas with the same density, respectively. This electron localization index has the advantage that it can be varied between 0 and 1 without any loss of information. The upper limit indicates perfect electron localization. A value of 0.5 corresponds to the reference system limit, i.e. a system of noninteracting fermions (homogeneous electron gas). Some years ago, Savin et al. [34] showed that the term D_σ has the physical meaning of the excess local kinetic energy density due to Pauli repulsion. In other words, a space region characterized by a high probability to find electron pairs typically corresponds to the upper limit of the ELF, while a region where this probability is weak corresponds to the lower limit of this function.

The Silvi–Savin approach to chemical bonding [35] is based on a topological analysis of the gradient field of the ELF. This analysis achieves a partition of the space into basins of the gradient field maxima or attractors. Due to the physical definition of the ELF, these basins are divided into two main groups with specific chemical significance: the core and valence basins. An important distinction is made between valence basins according to their synaptic order, σ, which indicates the number of core basins that are connected to each of them. Typically, nonbonding valence basins are monosynaptic, while two-center or multicenter bonds correspond to polysynaptic ($\sigma \geq 2$) valence basins. Hence, this classification allows us to clearly distinguish two categories of chemical interactions: shared (covalent, metallic) or unshared (ionic, hydrogen or van der Waals) electron interactions characterized by the presence or the absence of a polysynaptic valence basin, respectively. An efficient visualization tool is constituted by *f*-localization domains, defining an isosurface $\eta(r) = f$ that encloses points for which the ELF is greater than f. These different domains will help us to localize the topological basins in three-dimensional space.

Finally, we shall use a particular nomenclature to describe our topological analysis. In particular, the terms C(X) and V(X) will indicate the core and valence nonbonding attractor basins, Ω, of atom X, respectively. A complete and detailed description of this nomenclature can be found in Ref. [36].

3 Results and discussion

In this study, six LnX_3 lanthanide trihalide molecules were considered in order to analyze the structural evolution with respect to the nature of the metal and halogen atoms. In principle, the topological analysis of the ELF is restricted to all-electron wavefunctions. Without explicit core electrons there is no core basin and it is therefore impossible to rigorously define the synaptic order of the valence basins. Nevertheless, the topological analysis of the ELF gradient field presented here has been done with pseudopotential wavefunctions. Recently, Kohout and Savin [37] showed that the topological analysis of the ELF can be extended in a straightforward fashion to calculations carried out with pseudopotentials. Though there is no valence basin with

large core pseudopotentials the number and the location of the valence basins is identical to the all-electron case. With small core pseudopotentials the external part of the core gives rise to a well-defined basin which shares separatrices with the surrounding valence basins; therefore, the analysis can be carried out safely.

Contour maps of the ELF for selected molecules in the plane defined by the nucleus of the lanthanide atom and two halogen nuclei are displayed in Fig. 1.

There is no local maximum between the lanthanide and halogen cores and therefore these lanthanide trihalide molecules appear to be purely ionic species. In the valence shell, the ELF local maxima are located on the external side of the halogen atoms. With respect to conventional ionic systems such as alkali halides, the most striking feature observed in Fig. 1 is the strong distortion of the lanthanide outer core shell. Similar distortions of the charge density Laplacian in external core shells have recently been reported by Bytheway and coworkers [38, 39] for alkaline-earth and transition-metal derivatives from period 4 and beyond. In their analysis of the charge density Laplacian there is no evidence for valence shell charge concentration but rather for charge concentrations in the outer core shell of the metal. This particular pattern of the core electron localization implies a strong distortion of the spherical outer core shell due to the ligand field. In the case of dicoordinated barium derivatives, Bytheway et al. [38] pointed out the tetrahedral arrangement of these core charge concentrations. In the case of the lanthanide trihalide molecules, a similar arrangement of the external core shell ($5s^2 5p^6$) charge concentration is expected and

Fig. 1. Contour maps of the electron localization function (*ELF*) for the optimized geometries of **a** LaF_3, **b** LuF_3, **c** $LaCl_3$ and **d** $LuCl_3$. The selected plane contains the lanthanide nucleus and two halogen nuclei. The variations occur between 0 and 1 (ELF dimensionless unit), increasing in steps of 0.01

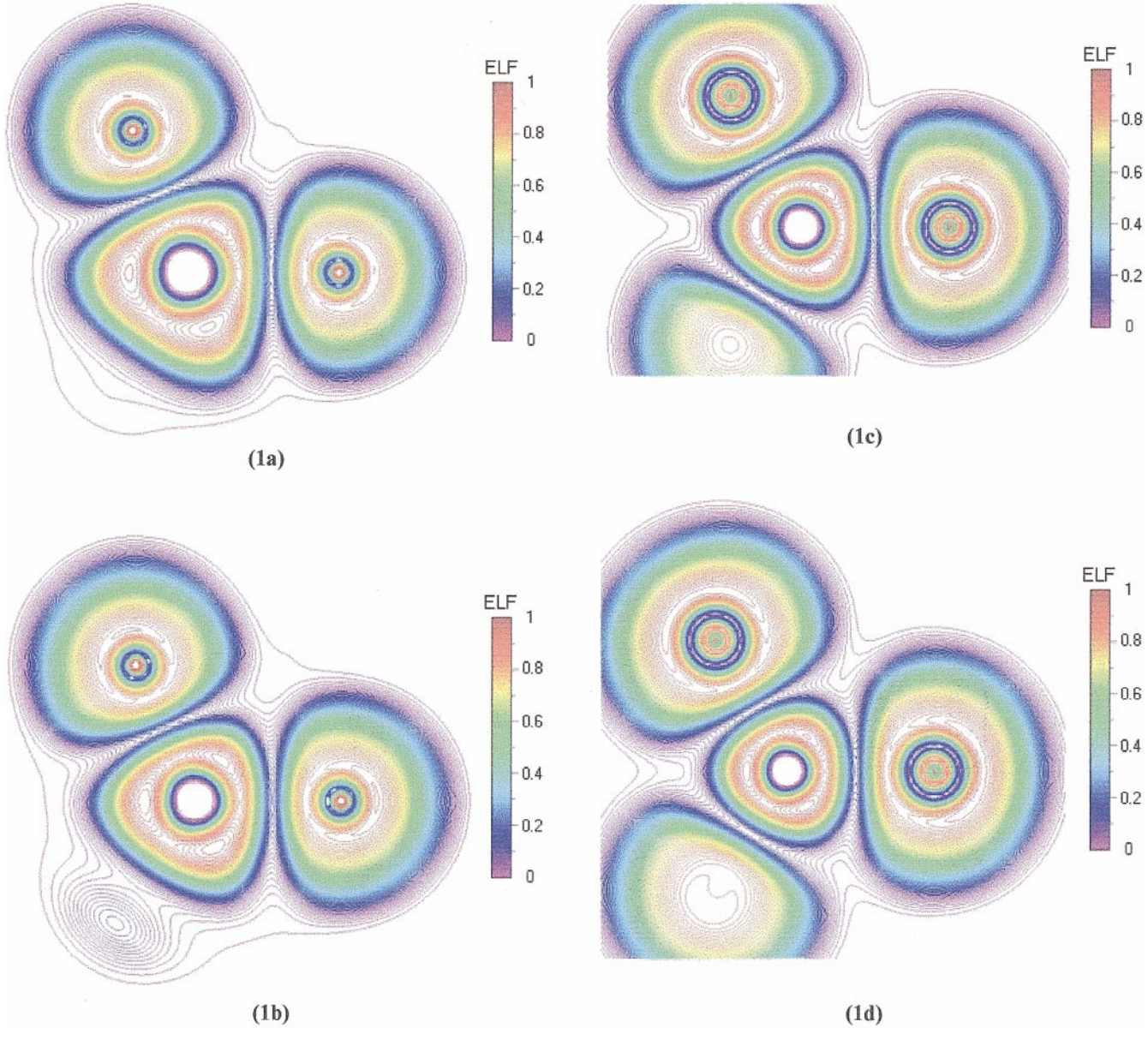

is evidenced by the ELF analysis as a consequence of the general homeomorphism that exists between the ELF and the charge density Laplacian gradient fields [40].

Intuitive arguments can be used to predict and explain the tetrahedral arrangement of the outer core basins of the central atom. As there are eight electrons in the external core shell and three ligands two structures can be reasonably expected: on the one hand, a C_{3v} structure and, on the other hand, a D_{3h} one. In the former structure there are four outer core shell basins, each with a population of the order of two electrons. The attractors of these basins occupy the vertices of a distorted tetrahedron, whereas the ligands are in front of three of the four faces of this tetrahedron. Such an arrangement of the attractors and of the ligands tends to minimize the Pauli repulsion between the outer core electrons of the metal with themselves as well as with the valence shell of the ligands. In the second structure (D_{3h} symmetry), the Coulombic repulsion between the anionic ligands is minimal. In this case, the outer core shell presents five basins organized in a trigonal bipyramidal structure, the ligands being in front of the edges of the basal triangle. This structure does not correspond to a minimum of the Pauli repulsion mostly because it possesses one core basin more than the C_{3v} one. Therefore, the structure of the lanthanide halide molecules results from competition between the minimization of the Pauli and electrostatic repulsions, which explains its evolution with respect to the nature of the metal and halogen atoms. Considering the lanthanide atom, the electron–nucleus potential increases with the atomic number. It tends to concentrate the charge density in the vicinity of the nucleus and its local spherical symmetry tends to preserve the atomic shell structure; therefore, the size and the polarizability of the lanthanide cores decrease along the series. The minimization of the Pauli repulsion favors a partition into basins either large enough to enable same-spin electrons to avoid one another or within which the integrated same-spin pair density is low, which implies that the basin populations do not noticeably exceed two electrons. Hence, for a given ligand, X, the X–Ln–X angle is expected to increase with the atomic number of Ln. With respect to the halogen anion one has to consider its size, its hardness and its polarizability. Again, the increase in the atomic number favors a planar geometry.

These expectations are verified by the calculations presented here. The localization domains of the selected LaF_3, LuF_3, $LaCl_3$ and $LuCl_3$ molecules for $\eta = 0.88$ are presented in Fig. 2.

This figure shows the lanthanide outer core basins surrounded by three valence nonbonding basins (halogens lone pairs) that mask the corresponding halogen core basins. The visualization of these localization

►

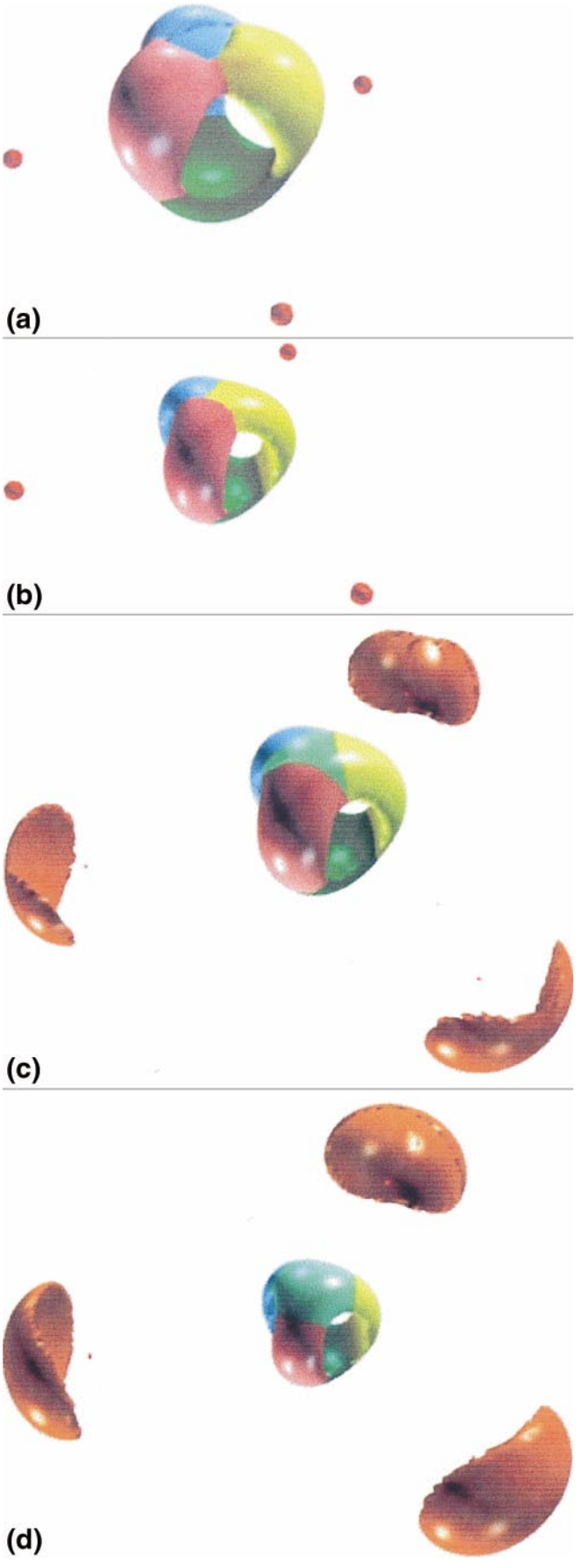

Fig. 2. Localization domains of the ELF, $\eta(r) = 0.88$, for the optimized geometries of **a** LaF_3, **b** LuF_3, **c** $LaCl_3$ and **d** $LuCl_3$. The valence monosynaptic attractor domains and the core attractor domains of the halogens are represented in *orange* and *red*, respectively. The outer core attractor domains of the metal are represented in different colors: *dark green*, *blue*, *pink*, *yellow* (and *light green* for the fifth core attractor domain of lanthanide trichloride molecules)

domains enables the metal core distortion to be observed distinctly, pointing out either a tetrahedral (fluorides) or a trigonal bipyramidal (chlorides) arrangement of the bulges of the outer core basins. As can be seen in Fig. 2a, the relatively high polarizability of the lanthanum atom results in a strong core shell distortion characterized by high values of the ELF in the neighborhood of the four attractors. This strong electron localization can also be observed near the nonbonding attractors in the valence shell of the fluorines. This phenomenon is a consequence of strong repulsive interactions occurring between the outer core electrons of the metal and the valence shell of the ligands; therefore, the ELF has rather weak values at the centers of the three faces occupied by the ligands which are (3, +1) critical points from a topological point of view (see Ref. [32] for more details). In the case of the LuF_3 molecule (Fig. 2b), the core distortion is weaker because the polarizability of this metal is smaller than that of lanthanum, while the smaller size of the lutetium core is responsible for the greater repulsions between the ligands. The importance of the nature of the ligands is illustrated by Fig. 2c and d, which should be compared with Fig. 2a and b, respectively. The strong repulsions between the chlorine atoms yield a planar or quasiplanar geometry for the chlorinated molecules. Consequently, the repulsions between the outer core electrons of the metal and the valence electrons of the ligands are weaker than for the corresponding fluorides. Thus, for a given metal, the core shell is less distorted in the chloride than in the fluoride, even in the case of $LaCl_3$ (Fig. 2c). Moreover, these quasiplanar structures are characterized by the appearance of a fifth outer core basin. This phenomenon can be described in terms of catastrophe theory concepts [41]. It typically corresponds to a plyomorphic step (appearance of a new attractor) that brings the system from a domain of structural stability to another one. It is worth noting that the ammonia inversion follows the same mechanism, though involving valence basins [41]. The interested reader can find a detailed description of these mathematical concepts applied to elementary chemical processes in Ref. [47].

This description of electron localization and repulsive interactions should explain the equilibrium geometries of these molecules. Recent theoretical studies [7, 8, 17, 18, 42–43] tend to confirm pyramidal equilibrium geometries for lanthanide trifluoride compounds. For example, we have recently obtained a 110°8′ bond angle for the LaF_3 molecule, tending towards the ideal limit of the 109°47′ characteristic tetrahedral angle. On the other hand, quasiplanar or planar geometries prevail for other molecules (chlorides), with a systematic increase in bond angles through the rare-earth series. The corresponding experimental data derived from gas-phase electron-diffraction measurements confirm these trends although trigonal shapes are also predicted for lanthanide trichloride molecules. Nevertheless, it is difficult to systematically compare quantum chemical calculations with experimental data. In particular, computational calculations yield an equilibrium geometry corresponding to a minimum of the Born–Oppenheimer potential-energy surface, while the electron-diffraction geometry results in a thermally averaged, effective structure. Moreover, due to shrinkage effects, it is well known that the symmetry of high-temperature molecules appears to be lower from this experimental technique than the calculated equilibrium symmetry. In other words, the experimental bond angles of planar LnX_3 molecules may appear to be smaller than 120° due to the puckering vibrations of these so-called "floppy molecules".

Besides a pure geometrical description of these molecular systems, a topological approach allowed us to get an insight into some of the physical properties of the selected molecules. These calculated properties for the selected lanthanide trihalide molecules are listed in Table 2 (see Ref. [36] for more details on the methodology). In particular, a topological basin population analysis was carried out by integrating the electron density over the topological basins. For practical considerations, we first considered a so-called C(*Ln*) "superbasin", gathering all the outer core basins of the metal.

This study indicates a systematic decrease in the electron population of the C(*Ln*) outer core basin of the metal through the lanthanide series. This steady progression corresponds to decreasing charge transfer from the ligands to the metal, i.e. a loss of approximately 0.1 electron from lanthanum to gadolinium derivatives and then again from gadolinium to lutetium derivatives. This phenomenon is directly related to the decreasing radius of the outer core shell of the metal and, therefore, to the decreasing size of the corresponding core basins. Hence, the decreasing volume of these basins limits the charge transfer from the nonbonding basins of the ligands to the outer core basins of the metal. Atomic charges can therefore be derived (Table 3), revealing increasing ionic character through the rare-earth series.

This result is consistent with the ionic description of the bonding pointed out by Adamo and Maldivi [18].

Table 2. Basin populations, $\bar{N}$, standard deviations, $\sigma(\bar{N},\Omega)$, and relative fluctuations, $\lambda(\Omega)$, of the topological basins, Ω, of selected lanthanide trihalide molecules

Molecule	Ω	$\bar{N}$	$\sigma(\bar{N};\Omega)$	$\lambda(\Omega)$
LaF_3	C(La)	8.66	1.02	0.12
	$C(F_i)_{i=1,3}$	2.14	0.62	0.18
	$V(F_i)_{i=1,3}$	7.63	0.87	0.10
GdF_3	C(Gd)	8.58	0.97	0.11
	$C(F_i)_{i=1,3}$	2.14	0.62	0.18
	$V(F_i)_{i=1,3}$	7.66	0.88	0.10
LuF_3	C(Lu)	8.49	0.92	0.10
	$C(F_i)_{i=1,3}$	2.14	0.62	0.18
	$V(F_i)_{i=1,3}$	7.69	0.88	0.10
$LaCl_3$	C(La)	8.69	0.98	0.11
	$C(Cl_i)_{i=1,3}$	10.06	0.71	0.05
	$V(Cl_i)_{i=1,3}$	7.71	1.08	0.15
$GdCl_3$	C(Gd)	8.59	0.97	0.11
	$C(Cl_i)_{i=1,3}$	10.06	0.71	0.05
	$V(Cl_i)_{i=1,3}$	7.74	0.96	0.12
$LuCl_3$	C(Lu)	8.50	0.97	0.11
	$C(Cl_i)_{i=1,3}$	10.06	0.71	0.05
	$V(Cl_i)_{i=1,3}$	7.77	0.88	0.10

Moreover, chemical intuition clearly suggests increasing ionicity for these molecules, corresponding to the increasing hardness of the metal. Furthermore, in spite of the electronegativity difference of the ligands, we can notice weak atomic charge differences between lanthanide trifluoride and trichloride species. We checked this particular point with different calculation parameters (i.e. different basis sets, functionals and pseudopotentials) and all our results confirmed this tendency. Nevertheless, these charge similarities are not surprising because of the typical ionic bonding properties of the selected metal molecules. Hence, the higher electron affinity of chlorine in comparison with that of fluorine, about 0.2 eV difference, may counterbalance the weaker electronegativity of chlorine and thus explains easily the observed atomic charge similarities. Finally, a careful examination of the relative electron fluctuations (Table 3) indicates weak fluctuations within the core superbasin of the lanthanides. A further crossed-exchange contribution analysis points out non-negligible fluctuations between the $C(Ln)$ and $V(X_i)_{i=1,3}$ basins. These fluctuations decrease through the rare-earth series, i.e. from 0.32 to 0.27 for lanthanide trifluoride molecules and from 0.30 to 0.26 for lanthanide trichloride molecules. Hence, these variations confirm the increasing ionic character for these molecular systems. Finally, we examined the population variations of the outer core basins of the metal separately. This detailed description is presented in Table 4 and the nomenclature used in Fig. 3.

In the case of lanthanide trifluoride molecules, we can notice, on the one hand, an irregular decrease in the population of the $C_1(Ln)$ outer core basin (located on the ternary axis of the molecule) through the rare-earth series. This phenomenon is magnified as we approach a catastrophe (bifurcation point), which is related to the transition from pyramidal equilibrium geometries to planar ones (the case of LuF_3 with $\theta = 116°$). On the other hand, we observe a "slight" increase in the population of the three other $C_i(Ln)_{i=2,4}$ symmetric core basins. This charge transfer between core basins is counterbalanced by a weaker charge transfer from ligands to metal, thus explaining the weak variations in the $C_i(Ln)_{i=2,4}$ populations. Another point of interest is the case of trichloride lanthanide molecules, corresponding to the other domain of structural stability (from quasiplanar to planar molecular structures). The population variations of the $C_1(Ln)$ core basin are quite similar: an important decrease in this population is clearly observed from lanthanum to lutetium derivatives. Moreover, due to the appearance and growing of a fifth $C_5(Ln)$ core basin, the populations of the three symmetric $C_i(Ln)_{i=2,4}$ core basins strongly decrease. The weak population of this latter basin in $LaCl_3$ ($\theta = 118.1°$) and $GdCl_3$ ($\theta = 118.8°$) indicates that these structures are in the neighborhood of the catastrophe. For heavier lanthanide elements, this population strongly increases as the

Table 3. Calculated atomic charges for selected lanthanide trihalide molecules

	Q_{metal}	$Q_{halogen}$
LaF_3	+2.34	−0.77
GdF_3	+2.42	−0.80
LuF_3	+2.51	−0.83
$LaCl_3$	+2.31	−0.77
$GdCl_3$	+2.41	−0.80
$LuCl_3$	+2.50	−0.83

Table 4. Detailed description of the basin populations, $\bar{N}$, standard deviations, $\sigma(\bar{N},\Omega)$, and relative fluctuations, $\lambda(\Omega)$, of the outer core basins of the metal. The nomenclature used is described in Fig. 3

Molecule	Ω	$\bar{N}$	$\sigma(\bar{N};\Omega)$	$\lambda(\Omega)$
LaF_3	$C_1(La)$	2.24	1.08	0.52
	$C_i(La)_{i=2,4}$	2.14	1.04	0.51
GdF_3	$C_1(Gd)$	2.16	1.06	0.52
	$C_i(Gd)_{i=2,4}$	2.14	1.04	0.51
LuF_3	$C_1(Lu)$	1.83	1.01	0.56
	$C_i(Lu)_{i=2,4}$	2.22	1.06	0.51
$LaCl_3$	$C_1(La)$	2.13	1.06	0.53
	$C_i(La)_{i=2,4}$	2.05	1.05	0.54
	$C_5(La)$	0.41	0.59	0.86
$GdCl_3$	$C_1(Gd)$	2.10	1.06	0.54
	$C_i(Gd)_{i=2,4}$	2.00	1.04	0.54
	$C_5(Gd)$	0.49	0.64	0.83
$LuCl_3$	$C_1(Lu)$	1.51	0.96	0.61
	$C_i(Lu)_{i=2,4}$	1.84	1.02	0.56
	$C_5(Lu)$	1.47	0.95	0.62

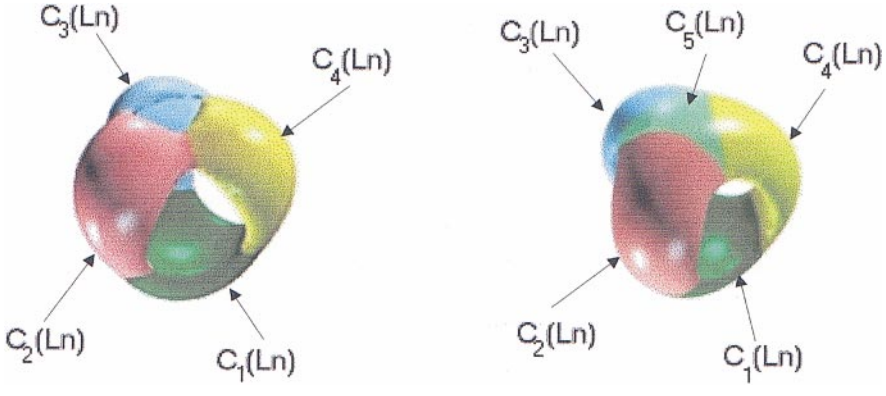

Fig. 3. Nomenclature used to describe the outer core basins of the metal. *Left*: tetrahedral arrangement of four core basins (trifluoride lanthanide molecules). *Right*: trigonal bipyramidal arrangement of five core basins (trichloride lanthanide molecules)

molecules tend to a planar geometry. We can finally notice that all these outer core basins are characterized by strong fluctuations, i.e. $\lambda > 0.5$. An analysis of the corresponding crossed-exchange contributions reveals that these fluctuations occur essentially between core basins and to a lesser extent with the valence non-bonding basins of the ligands.

4 Conclusion

The topological analysis of the ELF turns out to be an interesting alternative to classical molecular orbital studies. In this work, we have presented evidence for pure ionic *Ln–X* bonds for selected lanthanide trihalide molecules. Moreover, we have emphasized the increasing ionic character of these bonds from a quantitative point of view, which has not been seen in previous theoretical work. These results are in good agreement with the chemical concepts of hardness and softness. They testify to an accurate description of the molecular bonding properties and to a reliable partition of the space on the basis of physical arguments. On the other hand, this topological study has allowed us to point out the strong core distortion of the metal, favoring pyramidal geometries for these trihalide systems. Moreover, we have shown how this effect can be counterbalanced by increasing ligand repulsions due to the rare-earth contraction through the series. This physical description of electron pair arrangements, minimizing electron repulsions, has allowed us to introduce a new and clear explanation of the much debated pyramidal versus planar geometry of these molecules. Finally, we think that our accurate description of these heavy metal systems constitutes a solid base for further investigations, in particular for the establishment of more adequate force fields in future MM studies.

Acknowledgements. The authors thank Pascale Maldivi (C.E.A., Grenoble, France) for useful comments and discussions.

References

1. Cotton S (1991) Lanthanides and actinides. Macmillan, London
2. Gschneider KA Jr, Eyring JR (eds) Handbook on the physics and chemistry of rare earths, vols 1–28 (1978–1999) Elsevier, Amsterdam
3. Cecille L, Casarci M, Pietrelli L (1991) New separation chemistry techniques for radioactive waste and other specific applications; Commission of the European Communities. Elsevier London
4. (1998) Proceedings of the workshop GEDEON "Pyrochemical processes", Paris, France. CEA, Marcoule, France
5. Mottot Y (1986) Thesis. University of Paris VI, Paris
6. Zing C (1990) Thesis. University of Paris VI, Paris
7. Joubert L, Picard G, Legendre JJ (1998) Inorg Chem 37: 1984
8. Joubert L, Picard G, Legendre JJ (1998) J Alloys Compd 275–277: 934
9. Joubert L, Picard G, Legendre JJ (1998) Molten Salt Forum 5–6: 197
10. Gaune-Escard M (1996) In: Carlin RT, Matsunaga M, Selman JR, Deki S, Newman DS, Stafford GR (eds) 10th International Symposium on Molten Salts, vols 96-7. The Electrochemical Society, Pennington, p 439
11. Gaune-Escard M, Da Silva F, Rycerz L, Takagi R, Iwadate Y, Adya AK (1998) In: Trulove PC, De Long HC, Stafford GR, Deki S (eds) 11th International Symposium on Molten Salts, vol 98-11. The Electrochemical Society, Pennington, p. 627
12. (1976) Gmelin Handbuch der Anorganischen Chemie: Sc, Y, La und lanthanides. Springer, Berlin Heidelberg New York
13. Hargittai M (1988) Coord Chem Rev 91: 35
14. Dolg M, Stoll H (1996) In: Gschneider KA Jr, Eyring JR (eds) Handbook on the physics and chemistry of rare earths, vol 22. Elsevier, Amsterdam, p 607, and references therein
15. Myers CE, Norman LJ, Loew LM (1978) Inorg Chem 17: 1581
16. Lohr LL, Jia YQ (1986) Inorg Chim Acta 119: 99
17. Adamo C, Maldivi P (1997) Chem Phys Lett 268: 61
18. Adamo C, Maldivi P (1998) J Phys Chem A 102: 6812
19. Glendening ED, Weinhold F (1994) Theoretical Chemistry Institute Technical Report, WIS-TCI-803. University of Wisconsin. Press, Madison
20. Reed AE, Curtiss LA, Weinhold F (1988) Chem Rev 88: 899
21. Saxena KMS, Fraga S (1972) J Chem Phys 57: 1800
22. Ziegler T, Rauk A (1977) Theor Chim Acta 46: 1
23. Frisch MJ, Trucks GW, Schlegel HB, Gill PMW, Johnson BG, Robb MA, Cheesman JR, Keith TA, Petersson GA, Montgomery JA, Raghavachari K, Al-Laham MA, Zakrzewski VG, Ortiz JV, Foresman JB, Cioslowski J, Stefanov BB, Nanayakkara A, Challacombe M, Peng CY, Ayala PY, Chen W, Wong MW, Andres JL, Replogle ES, Gomperts R, Martin RL, Fox DJ, Binkley JS, Defrees DJ, Baker J, Stewart JP, Head-Gordon M, Gonzalez C, Pople JA (1995) Gaussian 94, version D.1. Gaussian, Pittsburgh, Pa
24. Becke AD (1988) Phys Rev A 38: 3098
25. Lee C, Yang W, Parr RG (1988) Phys Rev B 37: 785
26. Becke AD (1993) J Chem Phys 98: 5648
27. Dolg M, Stoll H, Savin A (1989) Theor Chim Acta 75: 173
28. Dolg M, Stoll H, Preuss H (1993) Theor Chim Acta 85: 441
29. Noury S, Krokidis X, Fuster F, Silvi B (1998) TopMod package. Laboratoire de Chimie Théorique, University of Paris VI, Paris. Available from http://www.lct.jussieu.fr
30. Joubert L (1997) ELF2D, version 2.0. Laboratoire d'Electrochimie et de Chimie Analytique, University of Paris VI, Paris
31. Pepke E, Murray J, Lyons J, Hwu TZ (1993) SciAn. Supercomputer Computations Research Institute. Florida State University, Tallahassee
32. Bader RFW (1990) Atoms in molecules: a quantum theory. Oxford University Press, Oxford
33. Becke AD, Edgecombe KE (1990) J Chem Phys 92: 5397
34. Savin A, Jepsen O, Flad J, Andersen OK, Preuss H, von Schnering HG (1992) Angew Chem Int Ed Engl 31: 187
35. Silvi B, Savin A (1994) Nature 371: 683
36. Savin A, Silvi B, Colonna F (1996) Can J Chem 74: 1088
37. Kohout M, Savin A (1996) Int J Quantum Chem 60: 875
38. Bytheway I, Gillespie RJ, Tang TH, Bader RFW (1995) Inorg Chem 34: 2407
39. Gillespie RJ, Bytheway I, Tang TH, Bader RFW (1996) Inorg Chem 35: 3954
40. Bader RFW, Johnson S, Tang TH, Popelier PLA (1996) J Phys Chem 100: 15398
41. Krokidis X, Noury S, Silvi B (1997) J Phys Chem A 101: 7277
42. Di Bella S, Lanza G, Fragalà IL (1993) Chem Phys Lett 214: 598
43. Lanza G, Fragalà IL (1996) Chem Phys Lett 255: 341